ELSEVIER

Polymer 41 (2000) 1589–1596

polymer

Morphology and properties of isotropic and oriented samples of cellulose fibre–polypropylene composites

A. Amash, P. Zugenmaier*

Institute of Physical Chemistry, Technical University Clausthal, Arnold-Sommerfeld-Str. 4, D-38678 Clausthal-Zellerfeld, Germany

Received 2 July 1998; received in revised form 19 February 1999; accepted 18 March 1999

Abstract

Thermal, morphological and dynamic mechanical properties of polypropylene (PP)–cellulose fibre (CF) composites were investigated. Two types of CF and a compatibilizer were used. Calorimetric measurements exhibited an increase in the crystallization temperature and crystallinity of the PP component. This is attributed to the nucleating effects of the fibre surfaces, resulting in the formation of transcrystalline regions observed by an optical method. The dynamic mechanical spectra of the composites revealed an increase in the stiffness and a reduction in the damping values with an increasing CF content. The results are consistent with morphological observations, which verify an improved interfacial adhesion between fibre and matrix. The effects of drawing on the structure and physical properties of PP–CF composites were also studied. Increasing draw ratio, the melting peak of PP component was shifted to higher temperatures suggesting a constrained melting, and the uniaxial elastic modulus was considerably enhanced. The biggest influence was observed for the samples of PP–spun cellulose and the lowest for neat PP. In addition to the fibrillar structure of the oriented PP, the highly CF orientation and the efficient compatibilization in composites are responsible for the effects observed in the drawn samples. © 1999 Elsevier Science Ltd. All rights reserved.

Keywords: Polypropylene; Cellulose; Drawing

1. Introduction

In recent years, a rapid growth occurred in the consumption of fibre reinforced polymer composites, yielding a unique combination of high performance, great versatility and processing advantages at favourable cost. Among other fillers used for such polymeric products, cellulose fibres (CF) became an important class of the reinforcing materials. They show many advantages, including low density, little damage during processing, little requirements on processing equipment, biodegradability, high stiffness and relatively low price [1–3]. However, the main disadvantage of cellulose filled polymer composites seems to be the incompatibility between the hydrophilic cellulose fibres and the hydrophobic thermoplastic (particularly, polyolefin) matrix. This may contribute to a poor stress transfer between the matrix and the filler, and a limited fibre dispersion in thermoplastic melt, leading to unsatisfactory final properties of the materials produced [4–6]. As a result, research efforts have been focused to find suitable coupling agents in the area of wood and cellulose reinforced thermoplastic composites, in order to overcome the problems mentioned [1–16]. Effects of the interfacial adhesion on the morphological characteristics and corresponding physical properties have been studied. Among other additives used for surface treatment and compatibilizing, maleic anhydride grafted polypropylene (MAPP) has been found very efficient in improving the filler dispersion and the compatibility in PP–CF composites [12–16].

The aim of this work is the study of the morphology, thermal and viscoelastic behaviour of isotactic PP reinforced with two types of cellulose fillers (short- and micro-fibres), and a small weight percentage of MAPP compatibilizer. Experiments are performed by means of dynamic mechanical thermoanalysis (DMTA), differential scanning calorimetry (DSC), scanning electron microscopy (SEM), polarization light microscopy and X-ray diffraction. Investigations on the structural and physical behaviour of drawn composites is an important part of the work. These studies provide valuable insights into the relationship between the properties of the composites considered in both isotropic and oriented states.

* Corresponding author. Tel.: +49-05323-72-2372; fax: +49-05323-72-2584.

PII: S0032-3861(99)00273-6

Table 1
Thermal properties of the undrawn materials investigated

Sample	T_c (°C)	T_m (°C)	ΔH_f (J g^{-1})	X_c (%)
(1) PP	112	161.5	100	52.5
(2) MAPP	112.5	160	100	–
(3) PP–15%MAPP	112.5	160.5	99.5	–
(4) PP–10% CFS	116.5	160	94	55
(5) PP–20% CFS	117.5	160.5	84	55.5
(6) PP–30% CFS	118.5	160.5	74.5	56
(7) PP–5% CFM	116.5	160.5	96	53
(8) PP–15% CFM	118	161.5	90.5	56
(9) PP–30% CFM	120	161	75	56.5
(10) PP–40% CFM	121	161	65	57
(11) PP–50% CFM	122	161	54	57
(12) -//- (without MAPP)	122.5	160.5	55	58

2. Experimental

2.1. Materials and sample preparation

Isotactic PP (P 5000; MFI = 1.5 g min^{-1} density $\rho = 0.902$ g cm^{-3}) supplied by the Hüls AG (Marl, Germany) served as a matrix material for the preparation of the composites. MAPP (Polybond 3150; 1.3 wt.% maleic anhydride) used as a compatibilizing agent was obtained from Vestolen GmbH (Gelsenkirchen, Germany). Chopped strands of spun cellulose fibres (CFS; Cordenka RT 700; $\rho = 1.4$ g cm^{-3}; length 8 mm) were supplied by Akzo Faser AG (Obernburg, Germany). Wood cellulose microfibres (CFM; Arbocel BE 600; $\rho = 1.5$ g cm^{-3}; length × thickness: 40×20 μm^2) containing >98.5% cellulose, were obtained from Rettenmaier GmbH (Ellwangen, Germany). Materials with fibre content ranging from 0 to 50 wt.% have been produced and tested.

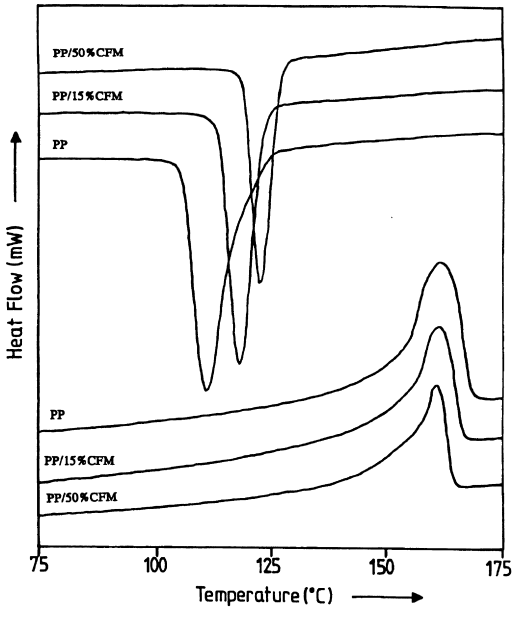

Fig. 1. DSC curves for crystallization and melting of neat PP and composites of PP–CFMs.

A Haake twin-screw extruder TW100 model (length × diameter: 745×240 mm^2) was used for the mixing and homogenizing of the CFs with the matrix material, PP, and a constant content (7 wt.%) of the coupling agent MAPP. The temperatures of the four zones of the extruder were 180, 190, 200 and 200°C, respectively. The screw speed was adjusted to 40 rpm.

The samples used for the different measurements were prepared by pressing the extruded granules in a hydraulic electrically heated press at 200°C for 10 min. After pressing, the samples (about 0.3 mm in thickness) were cooled (20°C min^{-1}) to room temperature under pressure.

For investigations on drawn samples, strip specimens of ca. 6 mm width were cut from the films and drawn at 148°C (±2°C) on a computer controlled tensile testing instrument. The drawing process was carried out at a speed of 5 mm min^{-1} achieving different draw ratios (λ). After drawing, the samples were immediately transferred into ice-water.

2.2. Measurements

A DSC-7 (Perkin–Elmer) served for calorimetric studies. The samples (each ca. 10 mg) were heated to 180°C and maintained at this temperature for 5 min. They were then cooled to 25°C at a rate of 10°C min^{-1}, held for 5 min at this temperature and heated again to 180°C at a rate of 10°C min^{-1}.

For drawn samples, the DSC melting curves were obtained by heating from 40 to 180°C at a rate of 10°C min^{-1}. Fractured surfaces of composite specimens were studied by using a Hitachi S-800 SEM operated at 25 kV. Optical micrographs of thin composite specimens (∽50 μm) were taken by using a BH-2 Olympus polarizing microscope. The films were prepared by the pressing procedure stated above.

X-ray diffraction with CuK_α was carried out on drawn samples using a flat film camera assembled on a Seifert generator. The distance between the sample and the recording film was about 6 cm.

Dynamic mechanical measurements were performed at a frequency of 10 Hz with the analyser Eplexor of Gabo Qualimeter (Ahlden, Germany). The samples of a 30×5 mm^2 area and a 0.3 mm thickness were cooled to ca. −150°C, and heated under a strain-controlled sinusoidal tensile loading to 170°C with a heating rate of 2°C min^{-1}. Measurements were taken every 2°C. The results presented in the figures and tables where checked on different samples and did not deviate more than 1% on an average or lie within the accuracy of the instrument or the method.

A detailed description of the experimental methods used, particularly the dynamic mechanical thermoanalysis, is given in Refs. [6,17].

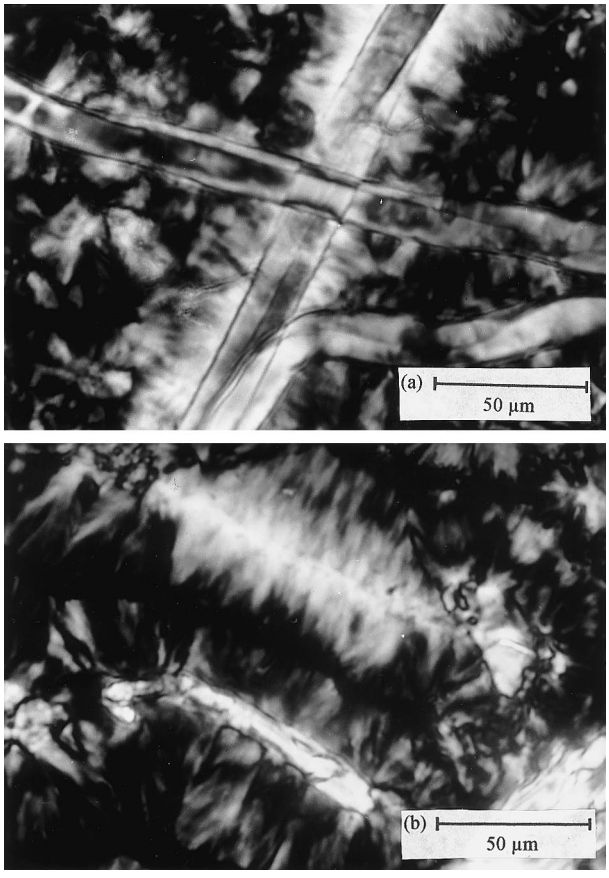

Fig. 2. Optical micrographs showing the transcrystallization in selected samples of (a) PP–30% CFS and (b) PP–30% CFM composites.

3. Results and discussion

3.1. Behaviour of isotropic samples

3.1.1. DSC measurements

The thermal parameters (crystallization temperature (T_c), melting temperature (T_m), heat of fusion (ΔH_f) and percentage of crystallinity (X_c)) determined and calculated from the differential scanning thermogrammes are summarized in Table 1. The fibre content is given as the weight percentage. The crystallinity of the PP component was determined by using the relationship

$$X_c(\%\ \text{crystallinity}) = \left(\frac{\Delta H_f}{\Delta H_f^0}\right)\cdot\left(\frac{100}{w}\right) \quad (1)$$

where a value of $\Delta H_f^0 = 190\ \text{J g}^{-1}$ was taken for 100% crystalline isotactic PP and w is the mass fraction of PP in the composite. Fig. 1 shows an example of a thermogramme for the melting and crystallization of neat PP and two PP–CFM composites.

The DSC results clearly show that the addition of small amounts of cellulose fibres (CFS and CFM) to PP, results in an increase of T_c of the polymer matrix. For the PP–CFM composites, a significant T_c—increase can also be detected with increasing filler content. The effects observed can be explained by the assumption that the cellulose fibres act as efficient nucleating agents for the crystallization of PP.

With regard to the melting temperature of the different samples investigated, the addition of cellulose fibres to PP causes only a marginal effect (±1°C), and no correlation of the results with the fibre content can be established (Table 1). The values of ΔH_f decrease in a regular manner for all the samples with increasing CF content, because the fibres act as a diluent in the PP matrix. However, a comparison of X_c of neat PP with the percentage of crystallinity calculated according to Eq. (1) for the PP component in the composites, shows clearly higher values for the samples with CF than for unfilled PP. This observation can again be explained that the fibre surfaces act as nucleation sites for the crystallization and the partial crystalline growth of PP. It may be assumed that the nucleating effect considerably contributes to the occurrence of transcrystalline layers around the fibres as shown in Fig. 2(a) and (b) representing optical micrographs for selected samples of PP–CFS and PP–CFM composites. It can be seen that somewhat dense crystallites have developed on the surfaces of the micro- and short-cellulosic-fibres.

In general, the transcrystalline morphology is characterized by a high density of nucleating crystallites which grow with an orientation perpendicular to the surface responsible for nucleation. In literature [18], the ability of different fibres and fillers to induce transcrystallinity in PP composites has been reported. For PP–cellulose composites, it has been stated that the pre-treatment of the cellulose surface with various chemicals inactivates the surface features, which are responsible for nucleating the transcrystallinity [19]. Other results, obtained by means of optical methods, have shown that the phenomenon of the transcrystallinity depends on the crystallization conditions of the polymer matrix [20]. However, the effects observed in this work under the measurement conditions chosen above, and by using the compatibilizer MAPP apparently indicate that the addition of CF to PP promotes the nucleation and a certain growth of the crystalline morphology of PP.

Table 2
Dynamic mechanical properties of isotropic samples

Sample	E' (MPa)/tanδ at 20°C	T_g (°C)/tanδ (at peak maximum)
(1) PP	1558/0.036	6.5/0.05
(4) PP–10% CFS	1788/0.033	6.5/0.043
(5) PP–20% CFS	2142/0.028	6.0/0.036
(6) PP–30% CFS	2725/0.025	6.5/0.032
(8) PP–15% CFM	1752/0.034	6.0/0.042
(9) PP–30% CFM	2093/0.031	7.0/0.036
(10) PP–40% CFM	2528/0.027	7.5/0.03
(11) PP–50% CFM	2863/0.02	7.0/0.024
(12) -//-(without MAPP)	2583/0.024	7.5/0.026

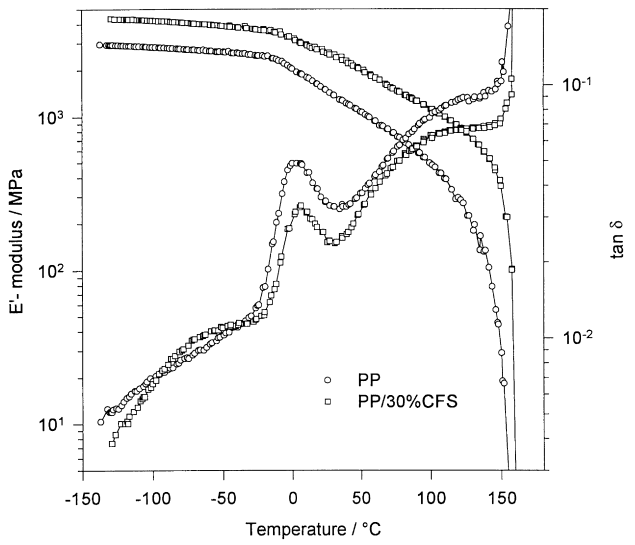

Fig. 3. Storage modulus (E') and damping factor (tanδ) as a function of temperature (DMTA spectrum) for neat PP and PP–30% spun cellulose short fibre (CFS) composite.

3.1.2. DMTA measurements

Some important data representing the dynamic mechanical behaviour of the investigated isotropic samples investigated are listed in Table 2. The composition of the materials is given in weight percentage. Fig. 3 depicts the dynamic mechanical spectra (storage modulus E' and loss factor tanδ as a function of temperature) for neat PP and a PP–CFS composite. Fig. 4 depicts the temperature dependence of the E' modulus (stiffness) and tanδ (damping) of PP–CFM composites with different compositions. The DMTA spectrum of the composite PP–50% CFM without MAPP (sample 12) is also recorded.

On the tanδ curve of PP (Fig. 3), three relaxations can be observed in the vicinity of -80°C (γ), 100°C (α) and at $T_g = 6$°C (β—glass transition). The origin of these transitions has been reported [21].

Comparing the DMTA spectra of neat PP and PP–CFS composite (Fig. 3), it becomes obvious that the addition of short fibres of spun cellulose to PP results in a remarkable increase of the stiffness and reduces the tanδ values of the material. While a significant decrease is detected for the intensities of both α- and β-relaxations, only a slight change can be observed for their shape and position. However, the E' curve displays an improved rubbery plateau indicating that the incorporation of CFS in PP induces reinforcement effects, which increase the heat-form and thermal–mechanical stability of the material at high temperatures. In comparison to neat PP, the tanδ curve of the composite which exhibits an additional low-temperature relaxation (at ca. -60°C) appears as a broad shoulder, and assigned to a rotary motion of the sequences ($C(6)H_2OH$) of cellulose [22]. It is noteworthy that the appearance of a relaxation process below the glass transition of the polymer matrix improves the toughness and the impact strength of the material at low temperatures [23].

For the DMTA spectra of PP–CFM composites (Fig. 4), it can be concluded that the viscoelastic properties of PP are considerably affected by adding CFM. The increase of CFM content (particularly for >30%) markedly enhances the material stiffness and reduces the corresponding damping values over a wide temperature range. An improvement of the rubbery plateau is indicated above the T_g of PP matrix. Comparing the DMTA spectra of the samples 11 and 12, it becomes obvious that the former (i.e. PP–50% CFM with MAPP) apparently shows higher stiffness and lower damping values than the latter without a compatibilizer.

Nevertheless, the small effects caused in composites without the addition of MAPP suggest that the hydrophobic part of a cellulose structure, clearly recognizable in the sheet-like conformation of a single chain, also contributes to the interfacial adhesion, but to a lesser extent than the hydrophilic part of the structure.

The clear improvement of the dynamic mechanical properties observed for all PP–CF composites, undoubtedly depends on the composition and individual component properties of the composites produced, but it is also affected by the strength and efficiency of the interfacial adhesion and interaction balance between the cellulose fibres and the bulk matrix. In literature [24], theories and mechanisms proposed to explain the phenomenon of adhesion between phases, have been reviewed.

For the composites investigated in this work, the occurrence of chemical bonding during compounding is assumed, since the functional group of the anhydride ring of MAPP is able to react chemically with the (OH)– groups of cellulose at the fibre surfaces [6,13,15]. In addition to the physical interactions, the resulting covalent and hydrogen bonds enhance the interfacial adhesion and the compatibilization between hydrophilic cellulose and hydrophobic PP, and improve the dispersion of the fillers in the matrix. Such

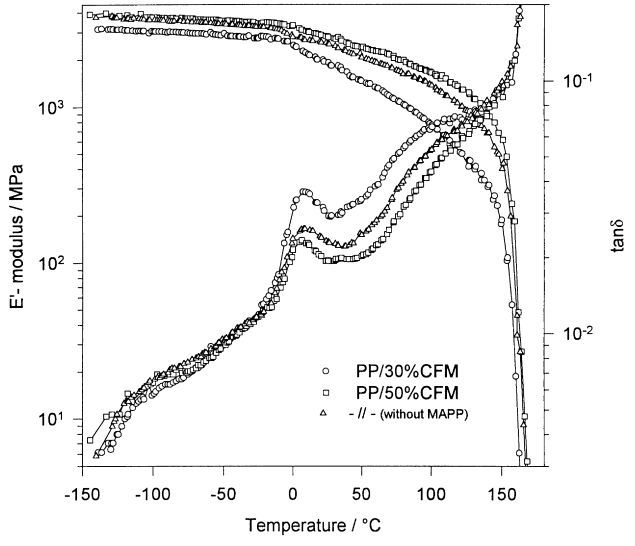

Fig. 4. DMTA spectra of PP–CFM composites for different compositions.

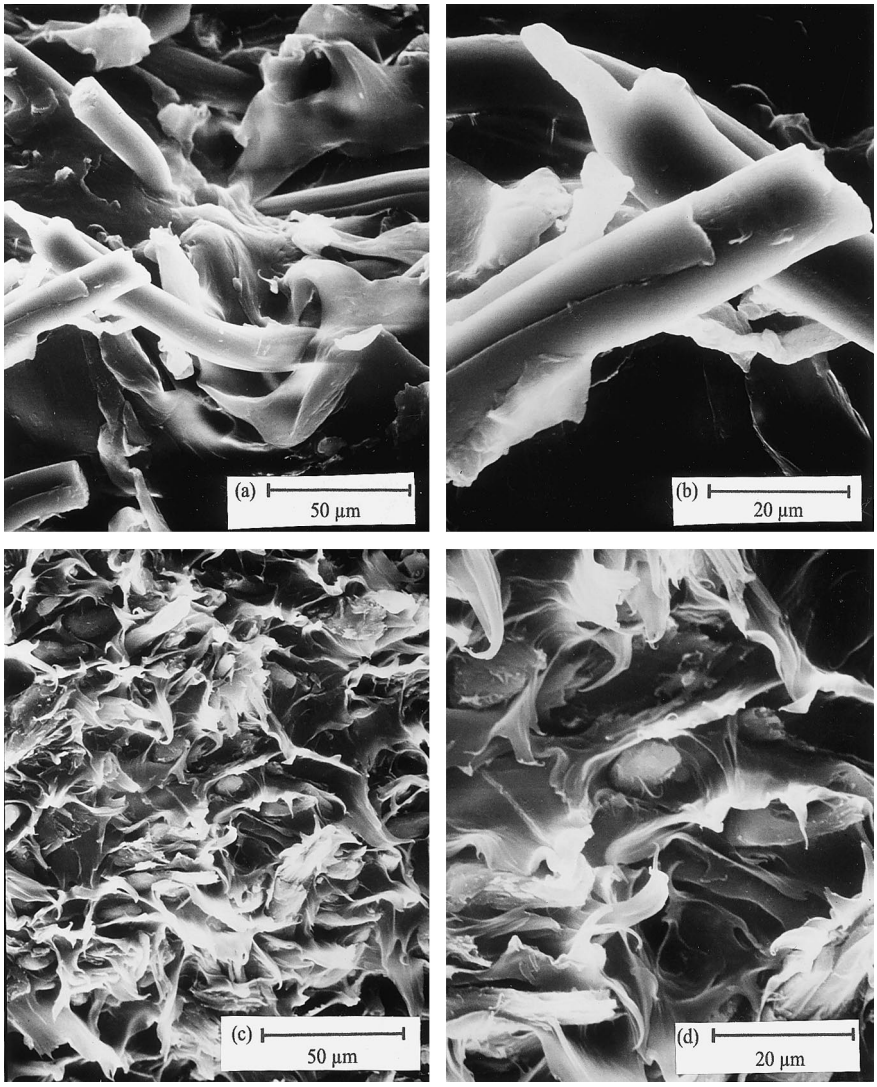

Fig. 5. Scanning electron micrographs of the fracture surfaces of the composites: (a) and (b) PP–30% CFS; and (c) and (d) PP–30% CFM (in both composite types 7 wt.% MAPP).

effects are crucial for the improvement of the mechanical properties of polymer composites.

The DMTA results obtained and interpreted above are largely confirmed by an investigation of the fracture surfaces (at room temperature) of the composite samples. SEM micrographs of different magnifications of the fracture surfaces are shown in Fig. 5(a)–(d): the composites PP + 30% CFS (Fig. 5(a) and (b)); and PP + 30% wood cellulose fillers (Fig. 5(c) and (d)). SEM micrographs provide evidence of good filler dispersion in the matrix, effective wetting of fibres by the matrix and strong interfacial adhesion between the components. In the presence of MAPP, no regions of particle agglomeration were seen in any of the investigated composite specimens. For PP–CFS composite, the entire fibres are clearly covered by layers of the matrix material that have been pulled out together with the CFs. The surface appearance implies great ductility. Also for PP–CFM samples, it can be seen that the fracture leaves a significant amount of matrix adhering to filler surfaces. These observations are consistent with the assumption that the MAPP compatibilizer is covalently bound to both the PP matrix and the CFs.

3.2. Effects of drawing

3.2.1. X-ray diffraction and melting behaviour

The X-ray diffraction patterns of the selected drawn samples of neat PP and both composite types are shown in Fig. 6(a)–(c). It is obvious, that neither CFS nor CFM yield any diffraction lines in addition to those of the polypropylene matrix. This may be due to the low crystallinity of the CFs used. The uniaxial orientation of PP crystallites takes place predominantly in the first stage of the drawing process, i.e. at relatively small draw ratios, represented by the arcing of the reflections. The increase of orientation results in a sharpening of diffraction arcs and spots. These

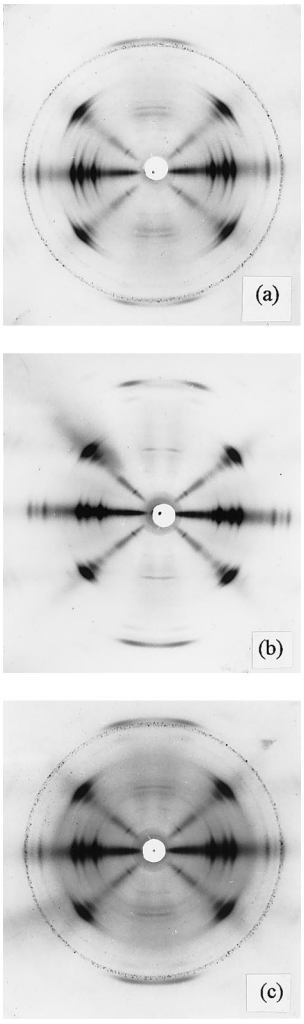

Fig. 6. X-ray fibre diffraction patterns of drawn samples: draw ratio $\lambda = 2.5$; grainy ring at d(spacing) = 3.155 Å used for calibration purpose; (a) PP; (b) PP–CFS; and (c) PP–CFM. The arcing of the reflections represents the goodness of orientation.

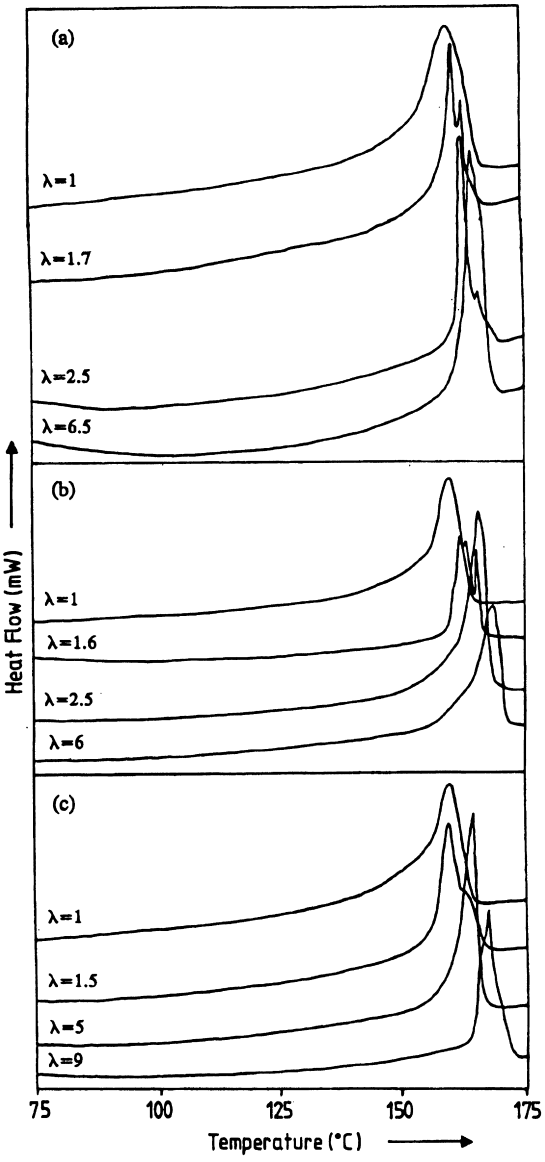

Fig. 7. The effect of drawing on the melting behaviour of various samples of: (a) neat PP; (b) PP–20% CFS; and (c) PP–40% CFM composites.

observations are consistent with the Peterlin model [25], stating that the drawing of semicrystalline polymers leads to a pronounced transformation of the spherulitic morphology into an extended fibrillar form. The resulting structure and properties are basically affected by the amount of taut-tie-molecules (TTM) and crystalline bridges, connecting crystal blocks along the fibre axis [26,27].

However, a comparison of the reflection characteristics (shape, intensity, etc.) observed for drawn samples of PP–CFS composite to those of PP–CFM and neat PP, shows that the orientation achieved for the former is higher than for the latter samples drawn at equivalent draw ratios. It may be assumed, that the stretched spun short-fibres contribute to a certain fixation of the degree of orientation achieved for the PP matrix, an effect determined by a good interfacial adhesion between the two components. CFM filler may have little influence on the orientation due to the small size of these fillers.

The DSC melting curves of several drawn samples of neat PP, PP–CFS and PP–CFM composites are shown in Fig. 7(a)–(c), beside those of the corresponding undrawn specimens. It can be seen that the drawing considerably affects the melting behaviour of the materials investigated, and in addition some differences between the curves can be established. Small draw ratios result in the appearance of an additional peak for neat PP, two peak maxima for PP–CFS and a broad shoulder for PP–CFM composite on the high temperature side of the melting peak of undrawn materials. Increasing the draw ratio, shifts the major endotherm peaks to higher temperatures and changes the additional peak-shoulder into a relatively marginal shoulder. It is noticeable, that the samples of the PP–CFS composite show the biggest increase in the melting temperature of the PP matrix, while the lowest increase is detected for the neat PP.

According to Samuels [28], two crystalline species are

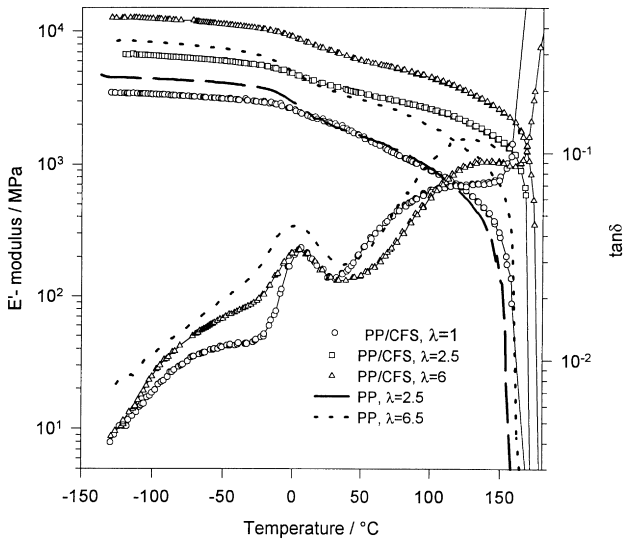

Fig. 8. The effect of drawing on the DMTA behaviour of PP and PP–20% CFS composite for different draw ratios.

involved in the source of the multiple-peak behaviour, either disordered crystals or crystals of different sizes.

However, a comparison of the DSC results obtained in this work for drawn samples of neat PP and composites obviously indicates, that the presence of the cellulose fibres (particularly CFS) considerably affect the melting behaviour of the polymer matrix, probably by fixation of oriented regions and the restriction of their partial relaxing, and results in constraint melting as observed for polyethylene [29] and polyethylene–aluminium composites [30]. These effects support the X-ray results and influence the mechanical behaviour discussed below. They are largely influenced by the interfacial adhesion between stretched fibres and polymer matrix.

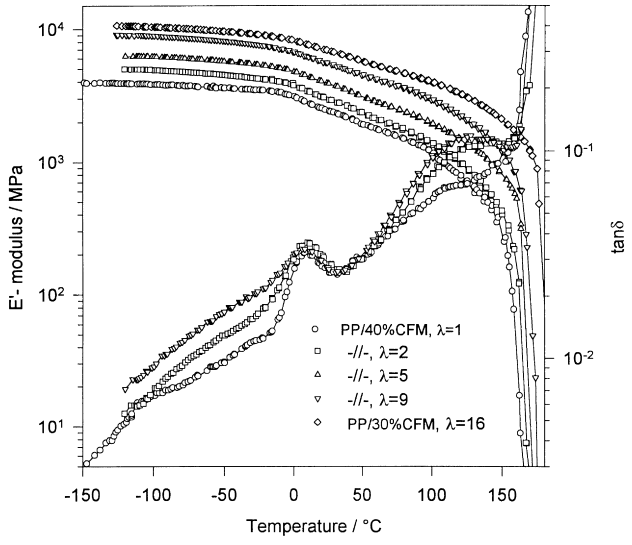

Fig. 9. Changes in DMTA spectra of drawn samples of PP–CFM composites.

3.2.2. DMTA properties

Fig. 8 depicts the temperature dependence of the E' modulus and tanδ for drawn samples of neat PP and PP–20% CFS composite. In Fig. 9, DMTA spectra are shown for oriented PP–CFM composites. Table 3 lists some selected dynamic mechanical data.

In comparison to the corresponding results of undrawn samples, first a drastic rise in the E' modulus is noted with an increasing draw ratio. The tanδ curves show over a wide low-temperature range a significant increase in damping values. The relative intensity of the relaxation of the glass transition is slightly decreased and a broadening of the assigned peak can be observed. The intensity of the crystalline α-relaxation is apparently increased and a corresponding peak or shoulder can now be detected easily. These effects are in particular attributed to the appearance of the fibrillar crystalline morphology in PP. However, the morphological reorganization involves also the non-crystalline phase, where the molecular mobility is considerably reduced due to the compression in the interfibrillar amorphous layers [31]. In a previous work [32], similar effects were observed on oriented PP and PP blends.

However, comparing the E' values detected for the different samples oriented at equivalent draw ratios, the increase in the stiffness of drawn PP–CFS composite is clearly higher than that of the other materials, where again the drawn samples of neat PP show a lower increase than those of the oriented PP–CFM composite. Moreover, the drop of the E' curves and the position of α-relaxation of PP–CFS samples are comparatively shifted to higher temperatures.

The difference detected in the dynamic mechanical behaviour of the materials investigated can be explained as follows: in the isotropic composite specimens, the CFs are well-dispersed in the PP matrix with a statistical distribution as detected by X-ray analysis. In addition to the orientation

Table 3
Dynamic mechanical data of drawn samples

Sample	Draw-ratio (λ)	E' modulus (MPa) at		
		20°C	75°C	150°C
(1) PP	1	1558	780	30
	2.5	2186	1289	129
	6.5	3863	2588	651
(2) PP–20% CFS	1	2142	1175	304
	1.6	3187	1837	751
	2.5	4085	3002	1500
	6	7503	5222	2602
	9	9215	6572	3125
(3) PP–40% CFM	1	2528	1568	250
	2	3091	1859	401
	3	3482	2052	595
	5	4015	2424	852
	9	5794	3435	1179
(4) PP–30% CFM	9	5616	3122	1019
	16	6984	4572	1746

occurring in the matrix component, the drawing causes a simultaneous axial stretch of the wetted fibres which become straight and oriented in the drawing direction. An additional tensile force acts along the drawing axis on the fibrillar PP matrix and results in a further increase of the composite stiffness. This explanation is more valid for PP–CFS than for PP–CFM composite, due to the big influence of the length and the good mechanical properties of spun cellulose used. However, the effects observed are also influenced by efficient interfacial interactions between fibres and matrix. These factors lead to an improvement of the stiffness and other properties, while the relaxation processes are probably affected by certain restrictions and a slight shift to higher temperatures occurs.

4. Conclusion

1. Calorimetric investigations show that the incorporation of CFs in PP causes an apparent increase in the crystallization temperature and percentage of crystallinity. These effects can be attributed to the fact that the surfaces of CF act as nucleating agents for the crystallization of the polymer, promoting the growth and formation of transcrystalline regions around the fibres.
2. The viscoelastic behaviour of PP is considerably affected by the presence of CFs. An increase in the E' modulus and reduced damping values can be observed with increasing fibre content due to reinforcement effects and interfacial adhesion between fibres and matrix. However, the influence of CFSs is greater than that of wood CFMs.
3. The drawing of neat PP and PP–cellulose composites apparently affects their structural, melting and viscoelastic behaviour. This is basically attributed to the characteristics of fibrillar morphology of the oriented polymer. However, the biggest influence is observed for the drawn samples of PP–CFS composite, while neat PP is less affected than PP–CFM. It may be concluded, that the fibre orientation together with the interfacial interactions greatly determine the drawing effects observed.

References

[1] Joly C, Kofman M, Gauthier R. J Macromol Sci 1996;A33(12):1981.
[2] Zadorecki P, Michell AJ. Polym Compos 1989;10:69.
[3] Beshay A, Hoa SV. Sci Engng Compos Mater 1992;2:86.
[4] Raj RG, Kokta BV, Daneault C. Int J Polym Mater 1989;12:239.
[5] Quillin DT, Caulfield DF, Koutsky JA. Int J Polym Mater 1992;17:215.
[6] Amash A. Doctoral thesis, Technische Universität Clausthal, D-38678 Clausthal-Zellerfeld, Germany, 1997.
[7] Zang YH, Sapieha S. Polymer 1991;32:489.
[8] Felix JM, Gatenholm P, Schreiber HP. Polym Compos 1993;14:449.
[9] Takasse S, Shiraishi N. J Appl Polym Sci 1989;37:645.
[10] Oksman K, Clemons C. J Appl Polym Sci 1998;67:1503.
[11] Clemons CM, Giacomin AJ, Koutsky JA. Polym Engng Sci 1997;37:1012.
[12] Woodhams RT, Thomas G, Rogers DK. Polym Engng Sci 1984;24:1160.
[13] Bataille P, Ricard L, Sapieha S. Polym Compos 1989;10:103.
[14] Joly C, Kofman M, Gauthier R. Compos Sci Technol 1996;56:761.
[15] Felix JM, Gatenholm P. J Appl Polym Sci 1991;42:609.
[16] Amash A, Zugenmaier P. Polym Bull 1998;40:251.
[17] Amash A, Zugenmaier P. J Appl Polym Sci 1997;63:1143.
[18] Folkes MJ. In: Karger-Kocsis J, editor. Polypropylene—structure, blends and composites, 3. London: Chapman & Hall, 1995.
[19] Quillin DT, Caulfield DF, Koutsky JA. J Appl Polym Sci 1993;50:1187.
[20] Felix JM, Gatenholm P. J Mater Sci 1994;29:3043.
[21] McCrum NG, Read BE, Williams G. Anelastic and dielectric effects in polymeric solids. London: Wiley, 1967 (New York: Dover Publications, 1991).
[22] Henze-Werthkamp H. Doctoral thesis, Technische Universität Clausthal, D-38678 Clausthal-Zellerfeld, Germany, 1993.
[23] Murayama T. Dynamic mechanical analysis of polymeric material. Amsterdam: Elsevier, 1978.
[24] Schulz J, Nardin M. In: Pizzi A, Mittal KL, editors. Handbook of adhesive technology, New York: Marcel-Dekker, 1994. p. 19.
[25] Peterlin A. J Mater Sci 1971;6:490.
[26] Peterlin A. J Appl Phys 1977;48:4099.
[27] Gibson AG, Davies GR, Ward IM. Polymer 1978;19:863.
[28] Samuels RJ. J Polym Sci Phys Ed 1975;13:1417.
[29] Smook J, Pennings AJ. Coll Polym Sci 1984;262:712.
[30] Thiele R. Doctoral thesis, Technische Universität Clausthal, D-38678 Clausthal-Zellerfeld, Germany, 1988.
[31] Candia F de, Botta A, Vittoria V. J Polym Sci Phys Ed 1986;24:2145.
[32] Amash A, Zugenmaier P. J Polym Sci Phys Ed 1997;35:1439.